Electronic Supplementary Material (ESI) for Analytical Methods.

Electronic Supplementary Material

A new electrochemiluminescence biosensor for detection of glucose based on polypyrrole/polyluminol/Ni(OH)$_2$-C$_3$N$_4$/glucose oxidase modified graphite electrode

Maryam Hamtak[a], Morteza Hosseini [b,c]1*, Lida Fotouhi [a]*, Mustafa Aghazadeh[d]

[a]*Department of Chemistry, Faculty of Physics and Chemistry, Alzahra University, Tehran, Iran*
[b]*Department of Life Science Engineering, Faculty of New Sciences & Technologies, University of Tehran, Tehran, Iran.*
[c]*Medical Biomaterials Research Center, Tehran University of Medical Sciences, Tehran, Iran*
[d]*Materials and Nuclear Research School, Nuclear Science and Technology Research Institute (NSTRI), P.O. Box 14395-834, Tehran, Iran*
E-mail address: smhosseini@khayam.ut.ac.ir, lfotouhi@alzahra.ac.ir

*Corresponding Authors:

Morteza Hosseini Center of Excellence in Electrochemistry, Faculty of Chemistry, University of Tehran, Tehran, Iran, E-mail address: smhosseini@khayam.ut.ac.ir

Lida Fotouhi, Department of Chemistry, *Faculty of Physics and Chemistry*, Alzahra University, Tehran, Iran, E-mail address: lfotouhi@alzahra.ac.ir

Electrochemical polymerization of luminol and pyrrole:

Electropolymerization of luminol can be performed by maintaining a suitable oxidation potential for the luminol monomer or by using cyclic voltammetry in a suitable positive scan potential region. As indicated in Figure S1 electropolymerization of luminol was performed either in acidic or buffered medium containing luminol, by cyclic voltammetry.

Figure S1

The pyrrole monomers were oxidized to free radicals on the electrode surface and linked each other to form dimer, tetramer and so on (Figure S2). The so formed hydrophobic clews during a chain propagation reaction resulted in the deposition of the Polypyrrole (Ppy) onto the electrode surface to form a film. Ppy have a linear structure and it linked only through α and α^1 positions of pyrrole ring. Pyrrole is oxidized to form radical cation which reacts with another pyrrole radical to form dimer. The dimer undergoes future oxidation and conjugation with pyrrole radicals. The procedure continues until Ppy is formed.

Figure S2

Preparation of nickel hydroxide-C_3N_4 nanohybride

Figures S3 (a to d) present the FE-SEM observations and EDS data of the electrosynthesized $Ni(OH)_2$-C_3N_4 nanohybride. For the deposited composite, clearly plate/sheet morphology is seen for the fabricated sample (Figures S3a and b). It is seen that the electro-synthesized nickel hydroxide has hexagonal plate texture as clearly seen in Figure S3b. Furthermore, the three dimensional structure is also observable for the carbons part of the fabricated nanohybride (Figure S3c). Notably, as clearly observable in Figure S3b, the nickel hydroxide plates are deposited and grown on the C_3N_4 part. The elemental analysis via EDS in

Figure S3c showed the presence of Ni, O, N and C elements in the composition of sample, with the weight percentages 38.07%, 44.02%, 8.78% and 9.14%, respectively. The presence of C and N elements in the prepared sample confirmed the C_3N_4 existence in the electro-synthesized nanohybride. Furthermore, the presence of Ni and O element in EDS data implicated the $Ni(OH)_2$ part of the fabricated $Ni(OH)_2$-C_3N_4 nanohybride.

Figure S3d shows XRD pattern of the fabricated $Ni(OH)_2/C_3N_4$ nanohybride powder. The typical diffraction peaks of β-$Ni(OH)_2$ (hexagonal structure, JCPDS no. 14-0117) i.e. (001), (100), (101), (102), (110), (111), (200), (103) and (201) are observed in the diffraction pattern of prepared sample planes. Furthermore, the diffraction related to the C_3N_4 is also seen at about 22.4°, which confirmed the formation of $Ni(OH)_2/C_3N_4$ nanohybride deposit on the cathode surface during our applied electrochemical platform.

Figure S3

Optimization of the performance of the ECL biosensor

The factors affecting performance of the biosensor towards glucose detection have been optimized: effects of pH, concentration of pyrrole, luminol, sulfuric acid and nanohybride ($Ni(OH)_2$-C_3N_4) on the intensity of ECL were investigated (Figure S4 to 8).

The following experimental conditions were found to give best results: A sample pH value of 8.6, number of scan for pyrrole and luminol were10 and 20, scan rate was 100 $mV.s^{-1}$, the concentration of H_2SO_4, pyrrole, luminol and $Ni(OH)_2$-C_3N_4 nanohybride were 0.16, 0.01, 0.005 $mol.L^{-1}$ and 1 $mg.mL^{-1}$, respectively.

For the use of this sensor, the pH condition is a crucial factor because the ECL reaction with hydrogen peroxide was a pH dependent process. The ECL response of glucose on the electrode in the pH range from 7.6 to 10.6 was investigated. Figure S4 shows the ECL intensity increased considerably with the rising of pH from 7.6 to 10.6. It was observed that at pH values more than 8.6, the ECL intensity of glucose response decreased and hence 8.6 was chosen as the optimum pH value and a phosphate buffer solution with this pH was used for the ECL determinations.

Figure S4

The effect of concentration pyrrole, luminol and sulfuric acid in the electropolymerization solution on the intensity of the ECL signal was also investigated. The intensity of the ECL signal in the presence of 50 $\mu mol.L^{-1}$ glucose was found to linearly increase with increasing the concentration of luminol from 1×10^{-3} $mol.L^{-1}$ to 5×10^{-3} $mol.L^{-1}$. Although further increase in the concentration of luminol (up to 5×10^{-3} $mol.L^{-1}$) cause enhancement in the intensity of the ECL biosensor and the ECL signal of luminol steadily decreased with increasing the concentration of luminol from 5×10^{-3} $mol.L^{-1}$ to 0.02 $mol.L^{-1}$. As shown in Figure S5, 6 and 7, for pyrrole, luminol and sulfuric acid, 0.01 $mol.L^{-1}$, 5×10^{-3} $mol.L^{-1}$, 0.16 $mol.L^{-1}$ were selected as the optimum concentration, respectively.

Figure S5, S6, S7

Also, the effect of the loading $Ni(OH)_2$-C_3N_4 nanohybride on the intensity of the ECL signal was studied by casting different amounts of $Ni(OH)_2$-C_3N_4 nanohybride on the surface of (Ppy-

Plu) composite. The amount of $Ni(OH)_2$-C_3N_4 nanohybride is a crucial factor influencing the oxidation of luminol.

Figure S8 illustrates the effect of the amount $Ni(OH)_2$-C_3N_4 nanohybride on the intensity of the ECL signal of luminol in the presence of 50 µmol.L^{-1} glucose. The ECL signal increased upon increasing the amount of $Ni(OH)_2$-C_3N_4 nanohybride and reached a desirable at 1mg of it in 1ml of ethanol. So, this ratio was used in the preparation of nanocomposite biosensor.

Figure S8

It is obvious that from Figure S9, with increasing the scan rate from 10 to 100 mV.s^{-1}, in cyclic voltammetry the current increased (Figure S9A) and showed that the anodic peak current increased linearly with $\nu^{1/2}$, revealing a diffusion controlled redox process. A linear relationship is established between the peak current and square root of the scan rate, justifying diffusion controlled reaction (Figure S9B). A scan rate of 100 mV.s^{-1} was selected for further experiments, since the maximum ECL sensitivity was observed at this value.

Figure S9 (A,B)

At the same time, the 5, 10, 15 and 20 cyclic numbers were done for electropolymerization of pyrrole and luminol. It showed that enhances the ECL signal up to 10 cycles for pyrrole and 20 cycles for luminol, then decreasing due to the absorption of the ECL emission because a greater amount of polymer is generated, so the surface of electrode to be insulated. However, the S/N ratio decreases after 10 and 20 cycles for pyrrole and luminol, leading to the selection of that number as working conditions. The enzyme electrode was prepared as explained in paper.

CV measurements were used to characterize the process of ECL biosensor modification. CV curves of stepwise modification of electrode in 1 mmol.L^{-1} $Fe(CN)_6^{3-}$/$Fe(CN)_6^{4-}$ containing 0.1

mol.L^{-1} KCl solution were shown in Figure S10 well-defined redox peak of $Fe(CN)_6^{3-}/Fe(CN)_6^{4-}$ was observed at bare graphite electrode(curve a) compare to the Ppy/Plu/$Ni(OH)_2$-C_3N_4 electrode (curve b). When GOx enzyme were coated on the electrode, the peak current markedly decreased (curve c), which demonstrated the GOx had been successfully immobilized on the electrode.

Figure S10

As showed in Figure S11, no detectable changes are observed in ECL intensity, when using the nanocomposite electrode in a 50 μmol.L^{-1} glucose solution in phosphate buffer (pH 8.6). The observed relative standard deviation was 3% under 10 consecutive potential scans (-0.2 to 1). So the ECL biosensor is stable during 80 second in 10 cycles without any decrease in reproducibility. The stability of sensor for before and after detection of glucose is the same. A little portion of the oxidized products of luminol may still remain on the electrode surface, reducing the effective surface. So it is found that applying successive (10 cycles) between −0.2 and 1.0 V by means of cyclic voltammetry in the buffer solution the fouling substances can be desorbed completely.

Figure S11

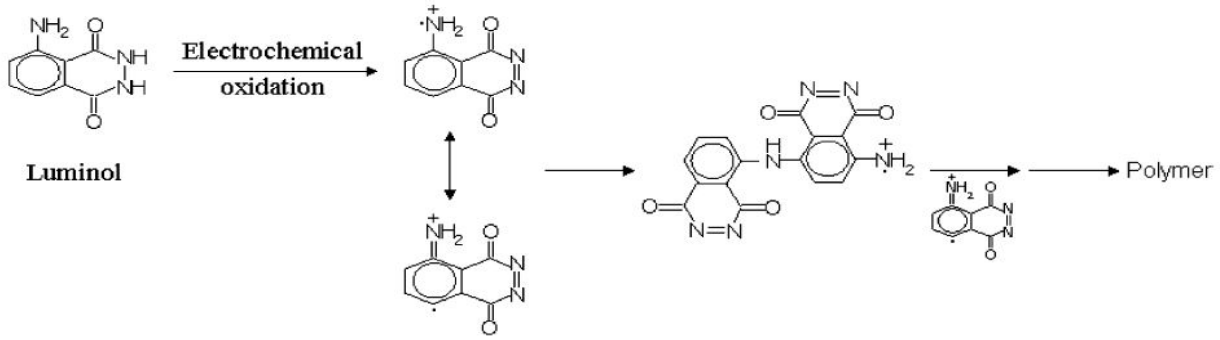

Figure S1. Simplified reactions involved in electrochemical luminol polymerization in acidic media.

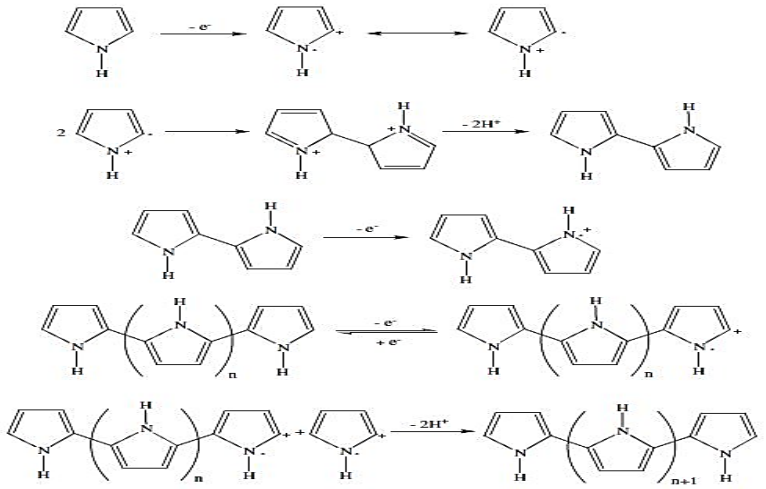

Figure S2. Simplified reactions involved in electrochemical pyrrole polymerization in acidic media.

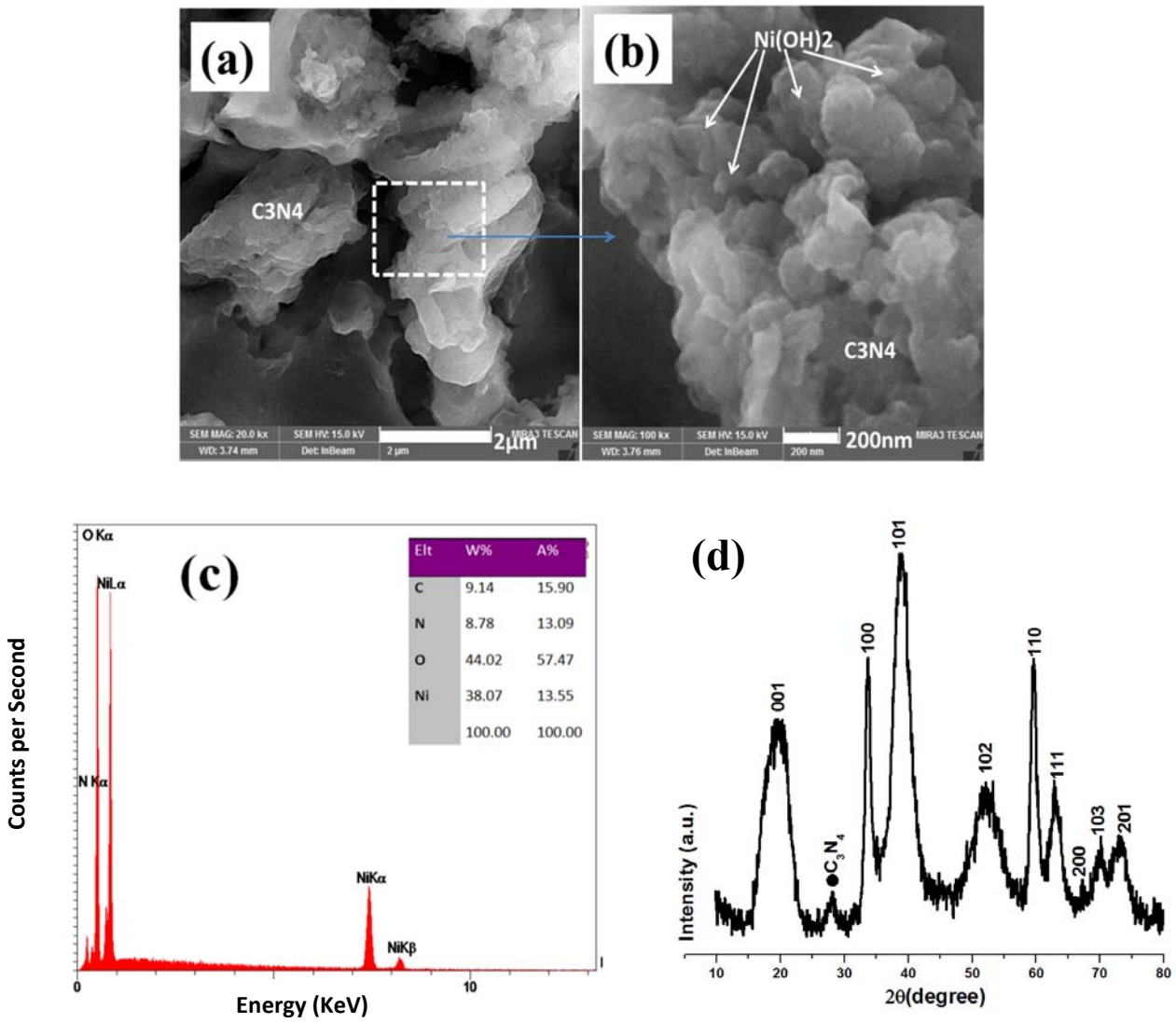

Figure S3. (a,b) FE- SEM images, (c) EDS graph and (d) XRD pattern of the prepared $Ni(OH)_2$-C_3N_4 nanohybride.

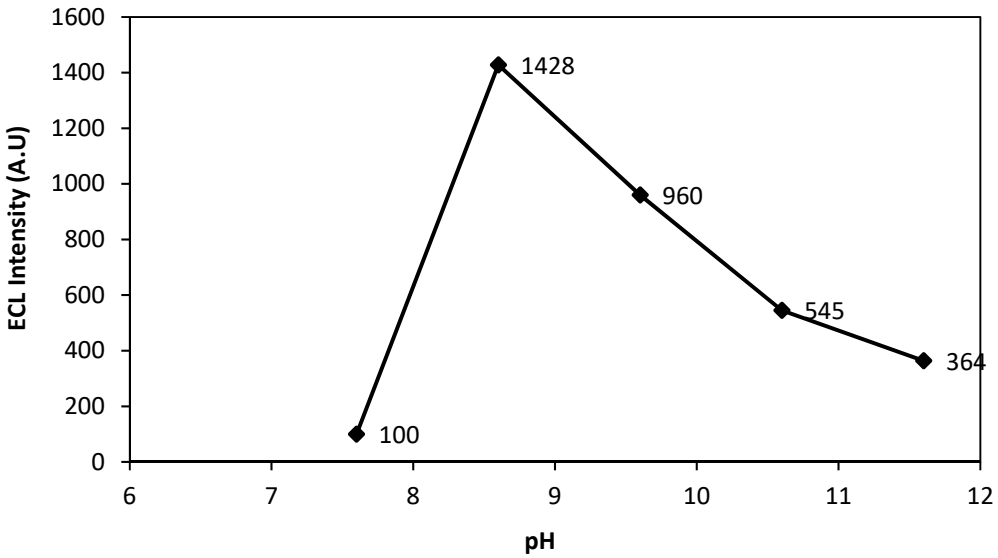

Figure S4. Effect of pH on the ECL signal assays carried out in: 0.1 mol.L^{-1} PBS, 50 µmol.L^{-1} glucose and scan rate 100 mV.s^{-1}.

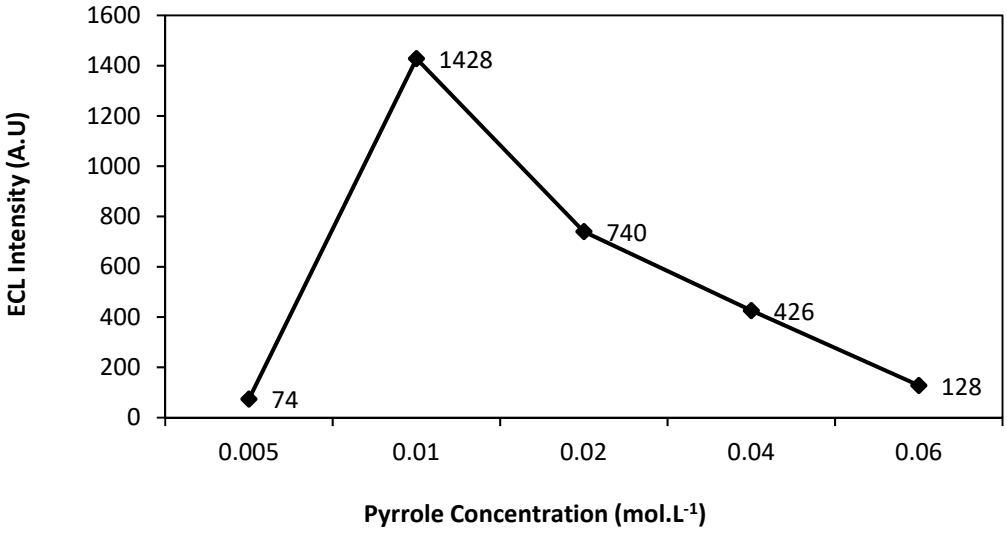

Figure S5. Effect of pyrrole monomer concentration on the ECL signal conditions: cyclic number of pyrrole: 10 and for luminol: 20, concentration of luminol: 5×10^{-3} mol.L^{-1}, assays carried out in: 0.1 mol.L^{-1} PBS (pH 8.6), 50 µmol.L^{-1} glucose and scan rate 100 mV.s^{-1}.

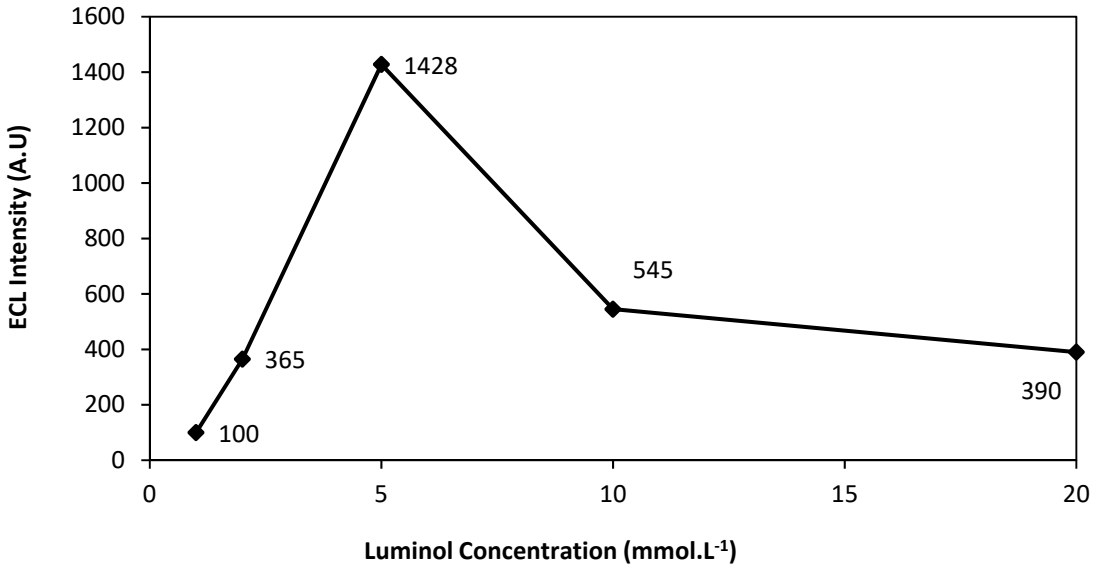

Figure S6. Effect of luminol monomer concentration on the ECL signal conditions: cyclic number of pyrrole: 10 and for luminol: 20, concentration of pyrrole: 1×10^{-2} mol.L^{-1}, assays carried out in: 0.1 mol.L^{-1} PBS (pH 8.6), 50 µmol.L^{-1} glucose and scan rate 100 mV.s^{-1}.

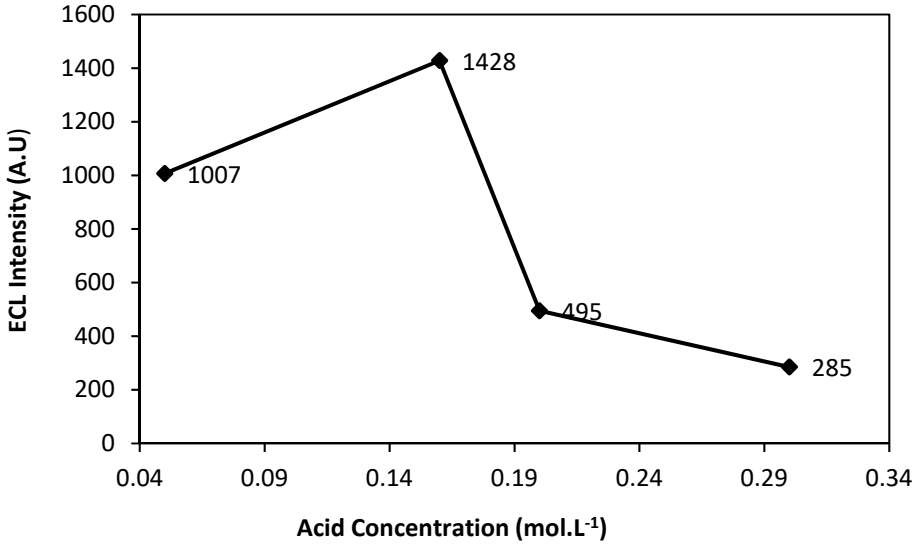

Figure S7. Effect of acid concentration on the ECL signal conditions: cyclic number of pyrrole: 10 and for luminol: 20, concentration of pyrrole: 1×10^{-2} mol.L^{-1}, luminol: 5×10^{-3} mol.L^{-1}, assays carried out in: 0.1 mol.L^{-1} PBS (pH 8.6), 50 µmol.L^{-1} glucose and scan rate 100 mV.s^{-1}.

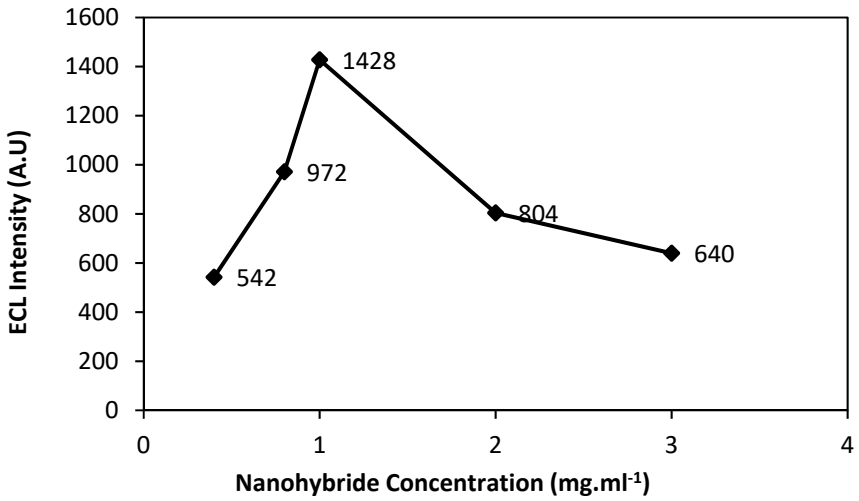

Figure S8. Effect of $Ni(OH)_2$-C_3N_4 nanohybride concentration on the ECL signal conditions: cyclic number of pyrrole: 10 and for luminol: 20, concentration of pyrrole: 1×10^{-2} mol.L^{-1}, luminol: 5×10^{-3} mol.L^{-1} and sulfuric acid concentration: 0.16 mol.L^{-1}; assays carried out in: 0.1 mol.L^{-1} PBS (pH 8.6), 50 µmol.L^{-1} glucose and scan rate 100 mV.s^{-1}.

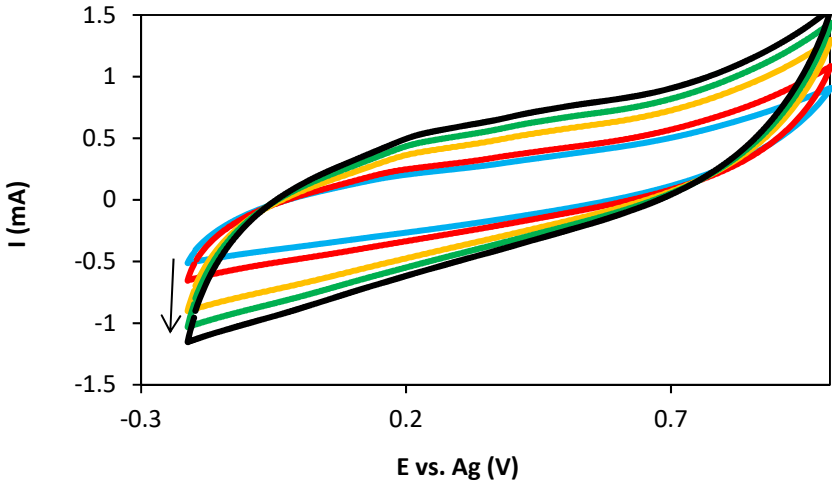

A

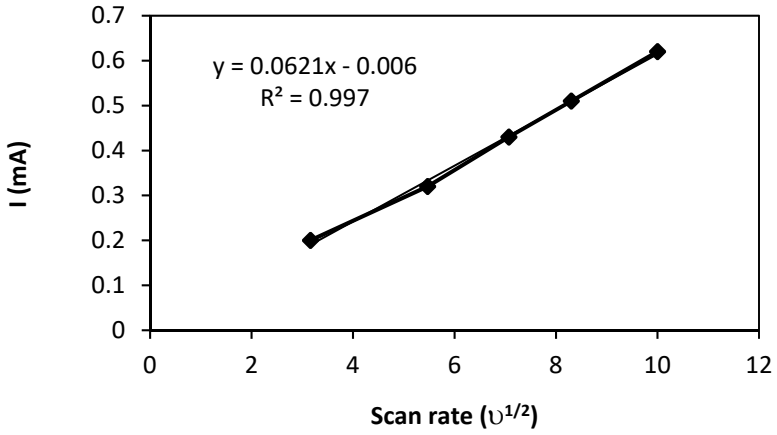

B

Figure S9.A. Effect of scan rate on the Ppy/Plu/$Ni(OH)_2$-C_3N_4/GOX in cyclic voltammetry Conditions: cyclic number of pyrrole: 10 and for luminol: 20, concentration of pyrrole: 10^{-2} mol.L^{-1}, concentration of luminol: 5×10^{-3} mol.L^{-1}, concentration of sulfuric acid: 0.5 mol.L^{-1}, assays carried out in: 0.1 mol.L^{-1} PBS (pH 8.6),) containing 50 µmol.L^{-1} glucose; potential range: -0.2 to 1 V; at different scan rate from bottom to top: 10, 30, 50,70, 100 mV.s^{-1}.

B. plots of peak currents *vs*. root of scan rate.

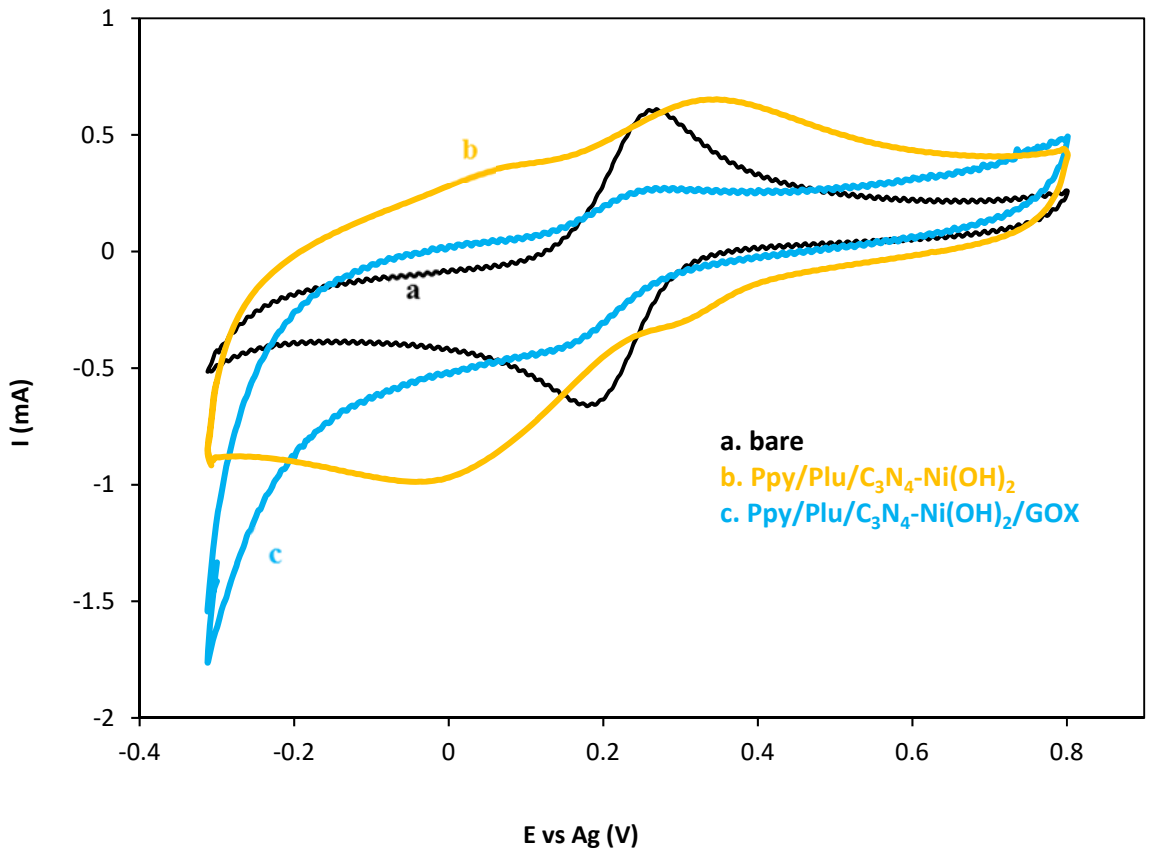

Figure S10. CV curves of bare-GE (black line), Ppy/Plu/$Ni(OH)_2$-C_3N_4-GE (orange line), Ppy/Plu/$Ni(OH)_2$-C_3N_4/GOX-GE (blue line) in 1×10^{-3} mol.L^{-1} $Fe(CN)_6^{3-}$/ $Fe(CN)_6^{4-}$ containing 0.1 mol.L^{-1} KCl solution. Scan rate: 100 mV.s^{-1}.

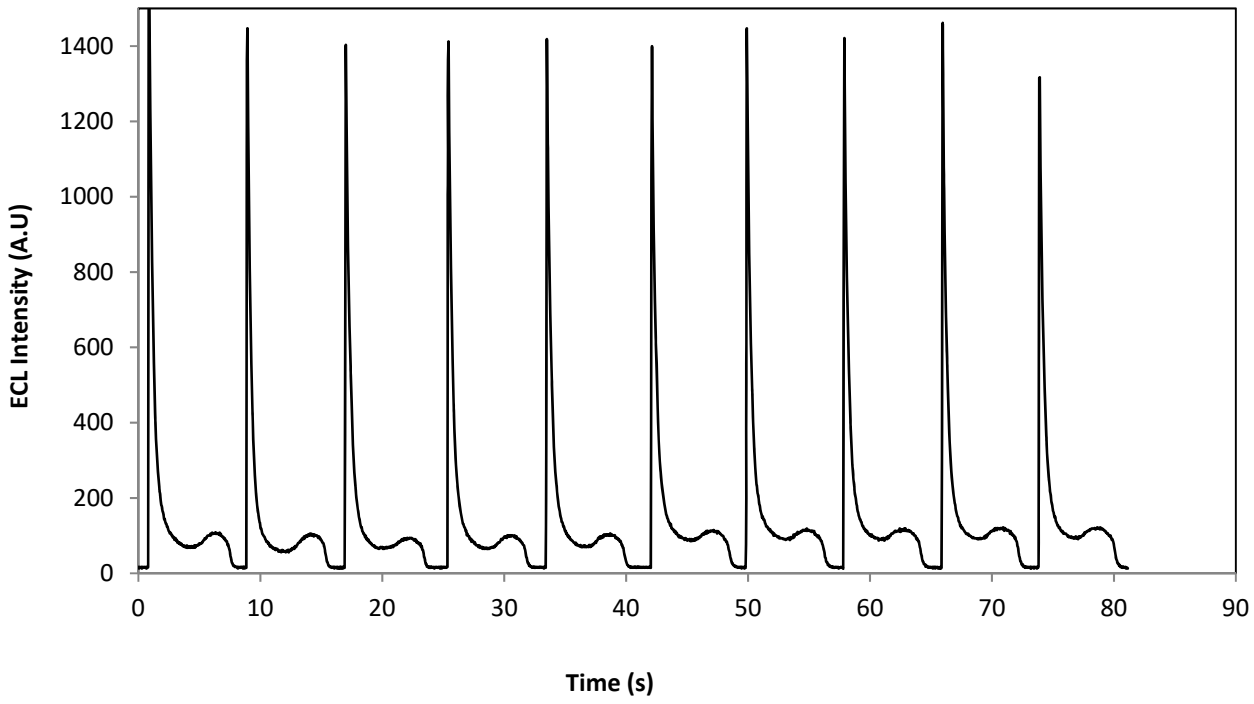

Figure S11. Reproducibility of (Ppy/Plu/$Ni(OH)_2$-C_3N_4/GOX) nanocomposite ECL intensity, Conditions: 0.1 $mol.L^{-1}$ PBS (pH 8.6) containing 50 $\mu mol.L^{-1}$ glucose; potential range: -0.2 to 1 V; scan rate =100 $mV.s^{-1}$.